Modeling of a Microstrip Line Referenced to a Meshed Return Plane

Ze Sun

EMC Laboratory Missouri University of S&T Rolla, USA sunz1@umsystem.edu

Jian Liu

Cadence Design Systems
San Jose, USA
jliu@cadence.com

Xiaoyan Xiong

Cadence Design Systems
San Jose, USA
xiongx@cadence.com

Yuan Liu

Cadence Design Systems
San Jose, USA
yuanliu@cadence.com

Victor Khilkevich

EMC Laboratory
Missouri University of S&T
Rolla, USA
khilkevichv@mst.edu

DongHyun Kim

EMC Laboratory Missouri University of S&T Rolla, USA dkim@mst.edu

Daryl Beetner

EMC Laboratory Missouri University of S&T Rolla, USA daryl@mst.edu

Abstract—Transmission lines referenced to meshed return planes are widely used because of the physical flexibility imparted by the meshed plane. Poor accounting for the meshed ground, however, can lead to severe signal integrity and radio frequency interference issues. Full-wave simulation can characterize the electrical performance at an early design stage, but it is both time and computational resource consuming. To make the simulation more efficient, a method is proposed in this study to model transmission lines with a meshed reference ground using 2D analysis. The 2D analysis is performed at several locations along the length of the trace above the meshed return to determine perunit-length RLGC parameters and partial self- and mutualinductances of the trace and meshed return. The partial selfinductance of the return is then corrected to account for the current direction along the mesh. Cascading the corrected S-parameters for each segment is then used to estimate the overall characteristics of the transmission line. Results found using this approach closely match those found with 3D fullwave simulation.

Index Terms—Meshed return plane, S-parameter, transmission line.

I. Introduction

In modern electronic devices, flexible printed circuit boards (FPCB) are widely used to accommodate compact sized designs. Physical flexibility of the board is enabled by introducing a meshed reference plane. In distinction to a traditional microstrip with a solid reference plane, the distribution and direction of the return current are determined by the geometry of the mesh reference plane. This affects the electrical performance of the transmission line. Hence, it is important to characterize the transmission line referenced to a mesh return plane accurately.

Because the transmission lines with a solid ground are translationally invariant, they can be modeled by 2D cross-sectional analysis [1], [2]. Due to the geometrical changes of the ground plane, however, strictly speaking,

only a full-wave simulation is applicable when modeling traces with a meshed reference plane [3]- [6], which is both time and computational resources consuming.

In this study, a method is proposed to calculate the *S*-parameters of a single-ended trace referenced to a meshed return plane using only 2D analysis. The periodic change of the structure and the position-dependent current flow direction are taken into account. This approach is time efficient and is validated by comparing with full-wave simulation results.

This paper is organized as follows. In section II, the initial characterization procedure is described. The cross-sectional geometries of the transmission line at different locations are extracted and simulated using a 2D solver. The resulting *RLGC* parameters can be cascaded to get the *S*-parameter of the whole board. For obvious reasons, however, the 2D analysis fails to capture the change of return current flow direction due to the geometry of the return plane. This leads to errors in the resulting *S*-parameters. In section III and IV, a method to modify the calculated self-inductance of the return plane obtained by the 2D analysis is proposed. In this way, the longer current flow path around the mesh openings can be handled correctly. The final result is validated through comparison with the 3D simulation.

II. SIMULATION METHODOLOGY

To demonstrate the proposed methodology, a single-ended signal trace referenced to a meshed return plane was simulated using a full-wave solver (CST [7]), as shown in Fig. 1. The total length of the line was 51.24 mm. The hatch width was 0.3 mm and the hatch pitch was 1 mm. On the left and right boundaries, the reference plane was solid with a length of 0.3 mm respectively to ensure continuity with the port modes. The trace

width was 0.25 mm and the air layer between the trace and reference plane had a thickness of 0.08 mm. The thicknesses of both trace and ground were 0.03 mm. The center of the trace was aligned with the center of the ground plane apertures. The nominal impedance of the transmission line (with a solid ground) is 67.7 Ω .

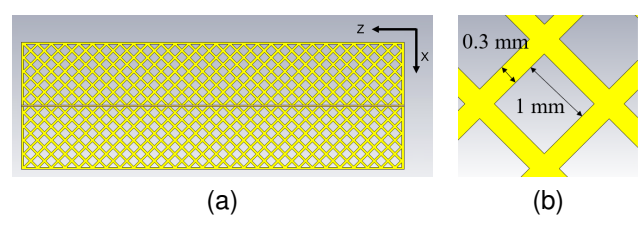


Fig. 1. (a): Top view of single-ended signal trace referenced to a meshed return plane. The x axis is along the vertical direction, the z axis is along the horizontal direction; (b): Zoomed-in view of the reference ground period.

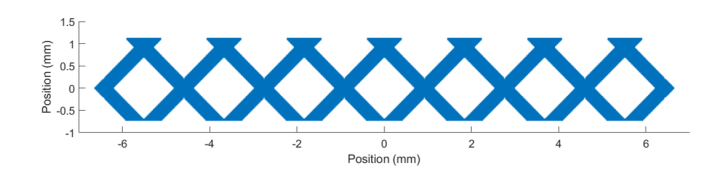


Fig. 2. One period of the meshed reference plane. The x axis is along the horizontal direction, the z axis is along the vertical direction.

The structure of one period of the meshed reference plane is shown in Fig. 2. Compared with Fig. 1, the coordinate system is rotated by 90 degrees for better viewing. The signal trace was located at x=0 mm. By taking cross-sections of the transmission line at multiple locations along the trace, a sampled representation of the changing geometry can be created. The distance between two adjacent cuts needs to be small compared with the size of the ground plane aperture such that the ground geometry can be appropriately sampled (segmented). By performing a 2D EM analysis using the cross-sectional geometries at the corresponding cuts, the per-unit-length (PUL) RLGC parameters of each segment can be obtained. By representing each segment as a translationally-invariant transmission line of length equal to the sampling step, the RLGC parameters of each segment can be converted to matrix parameters (S or *ABCD*). After this, the matrix parameters of the segments can be cascaded to obtain a matrix representation of the entire transmission line. This method, however, would lack accuracy.

To demonstrate this lack of accuracy, the mesh period in Fig. 1 was cross-sectioned at 64 locations, as shown in Fig. 3. The geometry was sampled with a step of 29.5 μm below the dashed line in Fig. 3 and 26.5 μm above the line respectively, which are less than 2% of the lattice period (1.84 mm). In this way, there are 49 cuts uniformly distributed around the aperture and 15 cuts uniformly distributed on the crosshatch intersection.

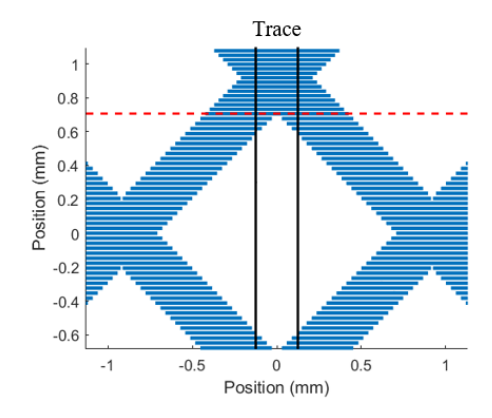


Fig. 3. Segmentation of the meshed round period. Only the portion closes to the signal trace is shown. The lower and upper portions of the lattice is divided by the red dashed line.

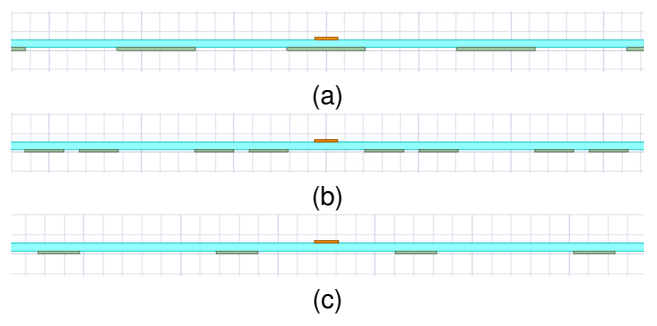


Fig. 4. The cross-sectional geometries at (a) cut 1, (b) cut 15, and (c) cut 25.

The cuts were indexed in ascending order from bottom to top. For example, cut 1 and cut 49 were located at the bottom and top vertices of the square hole, respectively, and cut 25 was located in the middle of the hole. Due to symmetry, the cross-section at cut i is identical to cut 50 - i where i is any integer between 1 to 24, and the cross-section at cut i is identical to cut i is any integer between 50 to 56. In this way, 33 cross-sectional analyses are required instead of 64. The cross-sectional geometries of several cuts are shown in Fig. 4. The *RLGC* parameters of each segment were simulated using the Ansys Q2D solver.

After calculating the *S*-parameters for one period, seventeen periods were cascaded to represent the entire transmission line in Fig. 1. The comparison of the transmission coefficient magnitude and phase (normalized to $50~\Omega$) obtained using the full-wave solver and by cascading the segments is shown in Fig. 5. As shown in the figure, the magnitude of the transmission coefficient is reproduced relatively well, but, the lines clearly have different electrical lengths (as can be seen from the phase progression), which can lead to discrepancies in the modeling of differential line skew modeling [8]. The mismatch is caused by the error in the inductance calculation, which is discussed in sections III-IV.

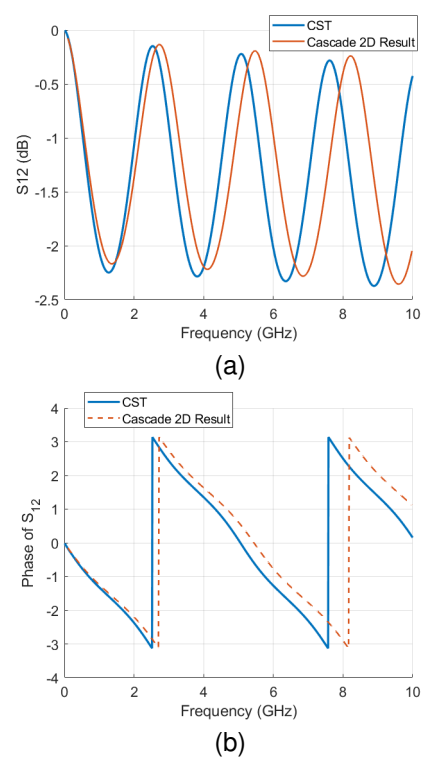


Fig. 5. Comparison of full-wave and segmented models: (a): Magnitude of S_{12} ; (b): Phase of S_{12} .

III. CURRENT FLOW PATH ON A MESHED RETURN PLANE

To investigate the error observed in the cascaded model, the surface current distribution on the top surface of the return plane produced by the full-wave solver is shown in Fig. 6. The trace center is located at x=0mm. When there is a conductor right underneath the trace, the return current flows predominantly along the z direction. When there is no conductor right underneath the trace, the return current flows predominantly along the edges of the apertures in the mesh returned plane, close to the trace. The qualitative difference between the translationally invariant line and the line with the meshed ground is illustrated in Fig. 7. For a segment of the translationally invariant line (7a) with length dz, the length of both trace and ground conductors is equal to the segment length: $dl_t = dl_g = dz$. Whereas for the line with the meshed ground (7b), the length of the conductor in which the current flows at the angle θ relative to the trace is longer: $dl_g = dz/cos\theta$. Our empirical hypothesis is that the contribution of the currents flowing at an angle to the total PUL inductance of the segments is larger than the contribution of the straight (vertical in Fig. 6 and 7) currents and is proportional to the length of the current path $dl_g = dz/cos\theta$. By calculating the contributions of the ground currents to the total PUL inductance and correcting it by the coefficient $K = 1/\cos\theta$, it is possible to improve the accuracy of the segmented

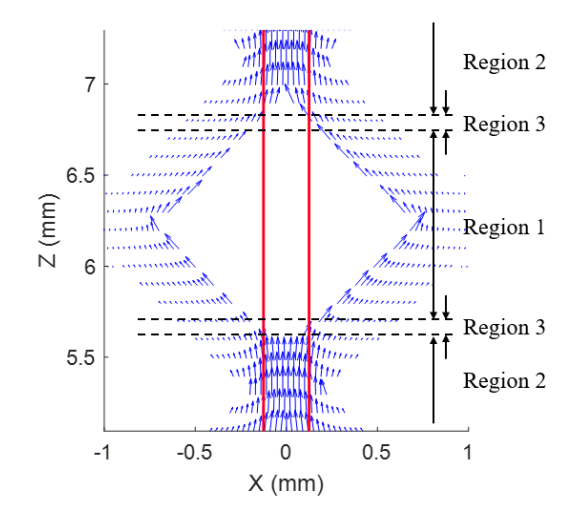


Fig. 6. Current density distribution on the top surface of the return plane. The vertical red lines indicate the position of trace.

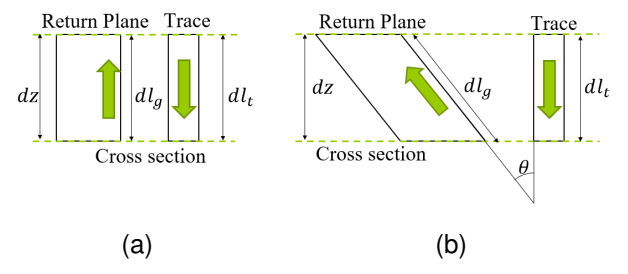


Fig. 7. (a): Assumed current flow direction in 2D analysis; (b): Top view of current flow direction in a mesh return plane.

representation of the transmission line with the meshed ground plane.

IV. Correction of the Inductance

2D solvers provide the value of the total PUL inductance of the cross-section. In order to perform the correction in the way described above, the contribution of the ground plane conductor needs to be found independent of the trace. This can be done by considering the magnetic flux \bar{B} in the TL cross-section. The value of the PUL L can be related to the energy stored in the magnetic field [1]:

$$L = \frac{1}{|I_0|^2 \mu} \int_S \bar{B} \cdot \bar{B}^* ds \tag{1}$$

Here μ is the permeability, I_0 is the total current in one of the conductors (trace or ground), S is the area of the cross-section, and \bar{B} is the magnetic flux density in the cross-section which is a superposition of contributions of the currents on the trace and on the return plane:

$$\bar{B} = \bar{B}_t + \bar{B}_g \tag{2}$$

By substituting (2) into (1), the inductance can be divided into the contributions of the trace L_t , ground L_g , and the mutual term L_m .

$$L = \frac{1}{|I_0|^2 \mu} \int_{S} (\bar{B}_t \cdot \bar{B}_t^* + \bar{B}_g \cdot \bar{B}_g^* + \bar{B}_t \cdot \bar{B}_g^* + \bar{B}_t^* \cdot \bar{B}_g) ds$$
 (3)

$$L_t = \frac{1}{|I_0|^2 \mu} \int_S \bar{B}_t \cdot \bar{B}_t^* ds \tag{4}$$

$$L_g = \frac{1}{|I_0|^2 \mu} \int_S \bar{B}_g \cdot \bar{B}_g^* ds \tag{5}$$

$$L_{m} = \frac{1}{|I_{0}|^{2} \mu} \int_{S} (\bar{B}_{t} \cdot \bar{B}_{g}^{*} + \bar{B}_{t}^{*} \cdot \bar{B}_{g}) ds$$
 (6)

$$L = L_t + L_g + L_m \tag{7}$$

After the inductance contributions are determined, the correction to the return-plane inductance can be made simply by multiplying the ground term by the correction coefficient $K = 1/cos\theta$:

$$L_g' = KL_g \tag{8}$$

A. Calculation of L_g

To calculate L_g according to (5), one needs to know the contribution of the ground current to the magnetic flux \bar{B} , which is typically not directly produced by the 2D solvers. However, it can be easily calculated by using the 2D formulation of the Biot-Savart law as:

$$\bar{B}_g(\bar{r}) = \frac{\mu_0}{2\pi} \int_C (\bar{J}dl) \times \hat{r}' \tag{9}$$

where \bar{r} is the radius-vector towards the observation point, \hat{r}' is the unit vector in the same direction, C is the contour of the conductor surface, and \bar{J} is the surface current density. The surface current can be obtained directly from the solver or from the H field at the surface of the conductor as $\bar{J} = \bar{H} \times \hat{n}$, where \hat{n} is normal to the conductor surface.

B. Calculation of the Correction Coefficient

As was said above, the correction coefficient *K* is used to account for the increased length of the current flow path on the meshed ground. This path increase, however, is not totally determined by the geometry of the meshed ground. As can be seen in Fig. 6 and Fig. 8, there are at least three qualitatively different regions of current flow. The current flows predominantly beneath the trace in region 1, predominantly along the edge of the opening in region 2, and there is a gradual change of the direction in region 3.

Calculation of the correction coefficient for regions 1 and 2 is straightforward: in region 1 it is equal to 1 and in region 2 it is equal to $1/\cos\theta$, where θ is the angle of the edge of the opening relative to the trace direction

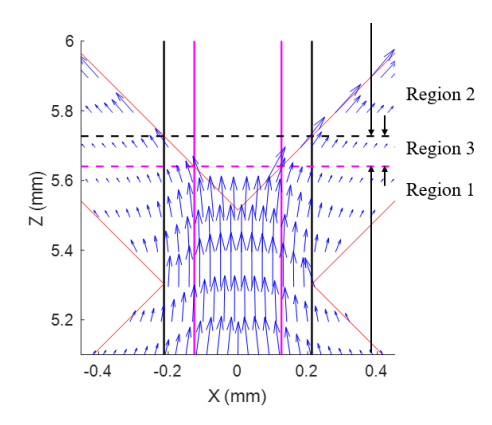


Fig. 8. Zoomed-in vire of Fig. 6 showing the boundaries between region 1, 2, and 3. The red lines are the edge of meshed ground. The pink lines indicate the edges of the trace. The black lines indicate the distance from "corner-to-corner" of the crosshatch intersection in the meshed ground.

(for our example that angle is equal to 45 *degrees* and the correction coefficient is equal to $\sqrt{2}$).

For region 3, θ changes from 0 to 45 *degrees*, and the value of *K* increases from 1 to $1/\cos\theta = \sqrt{2}$ accordingly. Here, we propose that *K* vary linearly over this region. The boundaries of region 3 are therefore determined by the entire geometry of the transmission line, not just the ground plane. Fig. 8 shows that in region 1, the return current predominantly flows underneath the trace, whose position is indicated by the two pink vertical lines. The upper boundary of region 1 is defined at the intersection of the trace outline and the edges of the ground plane opening. The lower boundary of region 2 is defined at the intersection of the lines (shown in black in Fig. 8) going through the vertices of the leftand right-hand-side openings relative to the trace and the edges of the next opening. The intermediate region 3 is defined between those boundaries. This definition is purely empirical and requires further refining especially for the cases when the trace width is large compared to the hatch pitch and the opening size, which is the subject of ongoing research.

The value of *K* for the transmission line model obtained as described above is shown in Fig. 9. Only the bottom portion of the aperture (from cut 1 to cut 25) is plotted. The corresponding value of *K* for the top portion of the aperture is symmetric.

C. Segment Cascading

After calculating L_g and K, the corrected value of the segment PUL inductance is calculated using (7) and (8) as:

$$L_{seg} = L - L_g + L'_g = L + (K - 1)L_g$$
 (10)

After cascading all segments together, the S-parameters of one mesh period are obtained. Further

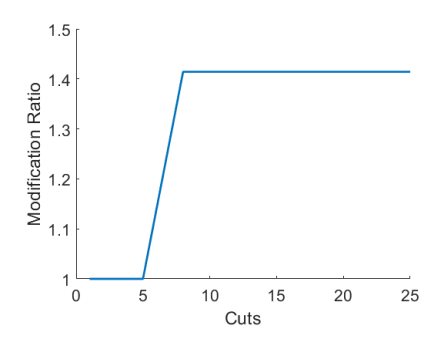


Fig. 9. Correction Coefficient, *K*, as a function of the cut, starting at the intersection of two mesh-lines (at cut 0).

cascading 17 units together, the S-parameters of the whole transmission line are calculated. The result is shown in Fig. 10. Comparing with the results in Fig. 5, the agreement between our model and the full-wave model is significantly improved. The values of S_{21} found with the proposed approach and full-wave simulations match closely along the entire curve, except where S_{21} is at a minimum and there is up to a 0.5 dB error between the two.

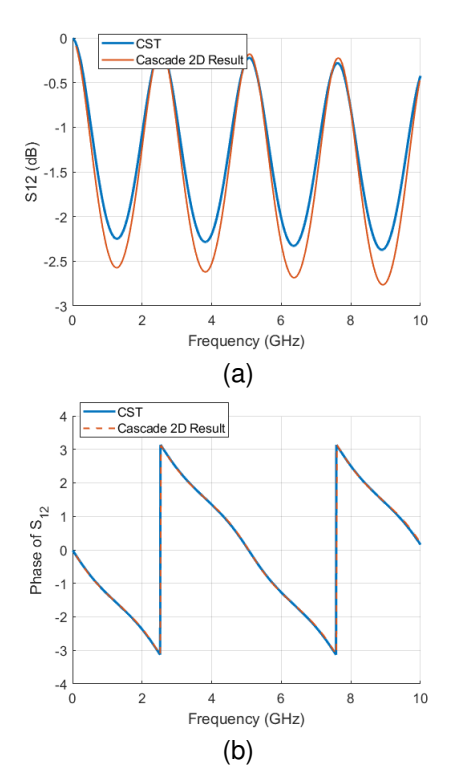


Fig. 10. Comparison between CST result and cascade result: (a): Magnitude of S_{12} ; (b): Phase of S_{12} .

V. Conclusion

To avoid a time-consuming 3D full-wave simulation, a method was proposed to model transmission lines over

a meshed ground plane using only 2D analysis. The gradual change of the mesh geometry along the trace is approximated by cutting the line at multiple locations. Each segment is characterized by performing the 2D analysis using the cross-sectional geometry at each cut. The value of the PUL L of each segment is corrected based on the ground geometry and surface current distribution. The S-parameters of the entire transmission line are obtained by cascading the segments. The result of cascading correlates well with the 3D full-wave simulation. The proposed method can aid in the design of FPCB. In the future, more cases with different geometries will be tested to validate the proposed method, including cases where the trace is shifted relative to the center of the ground plane opening and is routed at an arbitrary angle relative to the cross-hatch pattern.

VI. Acknowledgment

This work was supported in part by the National Science Foundation (NSF) under Grant IIP-1916535.

References

- [1] Pozar, D.M. 'Microwave engineering'. John wiley & sons. 2011. Ch.
- [2] Sun, Z., Liu, J., Xiong, X., Khilkevich, V., Kim, D. and Beetner, D., 2022, August. Extraction of Stripline Surface Roughness Using Cross-section Information and S-parameter Measurements. In 2022 IEEE International Symposium on Electromagnetic Compatibility & Signal/Power Integrity (EMCSI) (pp. 80-85). IEEE.
- & Signal/Power Integrity (EMCSI) (pp. 80-85). IEEE.

 [3] He, J., Hwang, C., Pan, J., Cho, G.Y., Bae, B., Park, H.B. and Fan, J., 2016, July. Extracting characteristic impedance of a transmission line referenced to a meshed ground plane. In 2016 IEEE International Symposium on Electromagnetic Compatibility (EMC) (pp. 651-656). IEEE.
- [4] Xiao, F., Murano, K. and Kami, Y., 2014, September. Modeling of differential line referenced to a meshed ground plane. In 2014 International Symposium on Electromagnetic Compatibility (pp. 735-740). IEEE.
- [5] Wu, S., Shi, H., Herndon, M., Cornelius, B., Halligan, M. and Fan, J., 2011, August. Modeling and analysis of a trace referenced to a meshed ground plane. In 2011 IEEE International Symposium on Electromagnetic Compatibility (pp. 137-141). IEEE.
- [6] Lee, H. and Kim, J., 2001, November. Electrical characteristics of single and coupled stripline on meshed ground plane in highspeed package. In Advances in Electronic Materials and Packaging 2001 (Cat. No. 01EX506) (pp. 261-267). IEEE.
- [7] CST Studio Suite 3D EM simulation and analysis software (2022), Dassault Systemes Simulia Corp. Accessed: Dec. 18, 2022.
- [8] Fan, J., Ye, X., Kim, J., Archambeault, B. and Orlandi, A., 2010. Signal integrity design for high-speed digital circuits: Progress and directions. IEEE Transactions on Electromagnetic Compatibility, 52(2), pp.392-400.